Journal of Alloys and Compounds 508 (2010) 71–78

Contents lists available at ScienceDirect

Journal of Alloys and Compounds

journal homepage: www.elsevier.com/locate/jallcom

Effects of quaternary alloying elements on the γ′ solvus temperature of Co–Al–W based alloys with fcc/$L1_2$ two-phase microstructures

Masahiro Ooshima, Katsushi Tanaka*, Norihiko L. Okamoto, Kyosuke Kishida, Haruyuki Inui

Department of Materials Science and Engineering, Kyoto University Sakyo-ku, Yoshidahon-machi, Kyoto 606-8501, Japan

ARTICLE INFO

Article history:
Received 28 June 2010
Received in revised form 6 August 2010
Accepted 13 August 2010
Available online 19 August 2010

Keywords:
Cobalt alloys
Phase separation
Thermodynamics
Ordering

ABSTRACT

The effects of quaternary elements on the γ′ solvus temperature of Co–Al–W based alloys with fcc/$L1_2$ two-phase microstructures have been investigated both experimentally and theoretically. The γ′ solvus temperature and partitioning behavior predicted by thermodynamic calculation agree well with those experimentally determined, indicating the usefulness of thermodynamic calculation in predicting the variation of the γ′ solvus temperature of Co–Al–W based alloys with quaternary elements. All investigated quaternary elements, except for Re, increase the γ′ solvus temperatures of Co–Al–W based alloys with varying efficiencies depending on quaternary element. Of the investigated quaternary elements, Nb, Ta and Ti are found to be the most effective in increasing the γ′ solvus temperature of Co–Al–W based alloys, which is consistent with the prediction from thermodynamic calculation. They have common thermodynamic characteristics that the ordering tendency with Co is high (but not significantly) and the phase-separation tendency with W is not so high.

1. Introduction

Since the efficiency of turbine engines for aerospace propulsion and land-based power generation increases with the increase in the combustion gas temperature, there have been ever-increasing demands for structural materials that can withstand severe oxidizing environments and high operating temperatures. Currently, Ni-based superalloys are the most widely used high-temperature structural materials for applications in aircraft engines and power generation systems operated at temperatures up to about 1350 K. These Ni-based superalloys generally exhibit two-phase microstructures consisting of the solid-solution based on Ni with a face-centered cubic (fcc) structure (designated the γ phase) and the stable $L1_2$-ordered intermetallic compound based on Ni_3Al (designated the γ′ phase). The γ/γ′ two-phase microstructure has been believed to lead to the excellent high-temperature mechanical properties of these Ni-based superalloys, and microstructure control (including the control of the partitioning behavior of alloying elements and the lattice misfit between the two phases) has been made through higher-order alloying in very sophisticated and elegant ways, in order to further increase the temperature capability of materials. As a result, the temperature capability of Ni-based superalloys has increased gradually year by year. However, the temperature capability has already increased almost to the upper bound limited by the melting temperatures of these alloys.

Recently, Sato et al. [1] discovered a stable $L1_2$ phase that can coexist with a fcc solid-solution based on Co in the Co–Al–W ternary system. They also reported that γ/γ′ two-phase microstructures that resemble those in Ni-base superalloys form in Co–Al–W ternary and some quaternary alloys. This discovery has opened up a pathway to the development of a new class of high-temperature structural material based on cobalt, 'Co-based superalloys'. Since the melting temperature of Co is higher than that of Ni by 40 K, Co-based superalloys have a possibility to achieve a temperature capability higher than that of Ni-based super alloys. Because of this expectation, mechanical and physical properties of Co–Al–W based alloys with γ/γ′ two-phase microstructures [1–4] as well as the constituent $L1_2$ phase [5,6] have been the subject of extensive studies in recent years. When investigated in compression and hardness tests, Co–Al–W based two-phase alloys exhibit excellent mechanical properties up to about 1050 K, but their strength rapidly decreases at higher temperatures. The rapid decrease in strength above 1050 K is believed to be due to the fact that the γ′ solvus temperature is rather low in Co–Al–W ternary alloys [3,4]. The γ′ solvus temperature of Co–Al–W ternary alloys is reported to be about 1273 K [1], which is by far lower than that (1613 K) of the third generation Ni-based superalloy, CMSX-4 [7]. Such a low γ′ solvus temperature of Co–Al–W based alloys has to be substantially improved when considering the expectation that Co-based superalloys have a possibility to achieve a temperature capability higher than that of Ni-based super alloys. Recent investigation by Shinagawa et al. [8] indicates that the $L1_2$ phase exists entirely from the Co side to the Ni side in the Co–Ni–Al–W quaternary system and that the γ′ solvus temperature increases from 1273 to 1473 K

* Corresponding author. Tel.: +81 75 753 5461; fax: +81 75 753 5461.
E-mail address: katsushi-tanaka@mtl.kyoto-u.ac.jp (K. Tanaka).

0925-8388/$ – see front matter © 2010 Elsevier B.V. All rights reserved.
doi:10.1016/j.jallcom.2010.08.050

almost linearly with the increase in the Ni content in the $L1_2$ phase. In addition, their research group also reported very recently that the addition of some transition metals such as Ta and Nb is beneficial to the increase in the γ′ solvus temperature of Co–Al–W based alloys [9]. The high-temperature strength is indeed observed to retain up to higher temperatures when Ta is added to Co–Al–W based two-phase alloys [3]. However, since the γ′ solvus temperature is generally known to vary with the volume fraction of the γ′ phase in the γ/γ′ two-phase field, more detailed studies are definitely needed to elucidate the effectiveness of each quaternary element to increase the γ′ solvus temperature of Co–Al–W based two-phase alloys.

In the present study, we investigate how the γ′ solvus temperature varies with the addition of quaternary elements both experimentally and theoretically. In the experimental approach, we determine the γ′ solvus temperature by thermo-mechanical analysis (TMA) through measurements of thermal expansion of the specimen made for quaternary alloys with compositions of Co–9 at.%Al–7 at.%W–2 at.%X (X = Sc, Ti, V, Cr, Fe, Ni, Hf, Zr, Nb, Mo and Re). In the theoretical approach, we carry out thermodynamic calculation using generalized thermodynamic interaction parameters among the constituent elements which are compiled in the literature [10]. We discuss the effectiveness of quaternary elements to increase the γ′ solvus temperature of Co–Al–W base alloys by comparing the experimental results with the results obtained by calculation.

2. Experimental procedure

Button ingots of ternary alloys with compositions of Co–9 at.%Al–*x* at.%W (*x* = 6, 7 and 8) and those of quaternary alloys with compositions of Co–9 at.%Al–7 at.%W–2 at.%X (X = Sc, Ti, V, Cr, Fe, Ni, Hf, Zr, Nb, Mo and Re) were prepared by arc melting in an argon atmosphere. These ingots were homogenized at 1523 K for 24 h in vacuum, followed by heat treatment at 1123 K for 96 h to allow precipitation of the γ′ phase. The γ′ solvus temperatures were determined by thermo-mechanical analysis (TMA) through measurements of thermal expansion of the specimen in an argon atmosphere at the heating rate of 10 K/min. Specimens used for TMA are rectangular parallelepiped specimens with the dimensions of about 2 mm × 2 mm × 10 mm cut from the heat-treated ingots. Microstructures of these specimens were examined with a scanning electron microscope (SEM) equipped with an energy dispersion X-ray (EDX) spectrometer. From the SEM images, the volume fractions of the constituent γ and γ′ phases are derived by measuring the area fractions of the phases.

3. Thermodynamic calculations

3.1. Method of calculations

We calculate γ′ solvus temperatures for quaternary alloys with compositions of Co–9 at.%Al–7 at.%W–2 at.%X (X = quaternary alloying elements), since microstructure observations has indicated that for Co–Al–W ternary alloys, the volume fractions of the γ and γ′ phases are almost identical with each other at the composition of Co–9 at.%Al–7 at.%W (as described later in Section 4). The compositions of the γ and γ′ phases in equilibrium in the two-phase region are Co–9 at.%Al–3.5 at%W and Co–9 at.%Al–10.5 at.%W, respectively. For the sake of simplicity, we carry out thermodynamic calculations for quaternary alloys with the assumptions described below.

(i) The enthalpy and entropy of the relevant phase are expressed with a point approximation, where the regular solution and Bragg–Williams models are adopted to describe atomic interactions and long-range order parameter, respectively.
(ii) The volume fractions of the γ and γ′ phases are unchanged upon quaternary alloying and are identical with each other.
(iii) The long-range order parameter for the γ′ phase is unity, meaning that Al and W atoms exclusively occupy B-sites of the $L1_2$ compound chemically described as A_3B.
(iv) Three different cases are considered in terms of the partitioning and site occupancy behavior of the relevant quaternary alloying element; (A) partitioned in the γ phase, (B) partitioned in the γ′ phase occupying A-sites, and (C) partitioned in the γ′ phase occupying B-sites.

The γ′ solvus temperature, which is defined as the transition temperature from the state of a mixture of the γ and γ′ phases (low-temperature state) to the homogeneous state of the disordered γ single-phase (high-temperature state), is estimated as the temperature at which,

$$\Delta G = G_{\mathrm{H}} - G_{\mathrm{L}} = 0 \tag{1}$$

where *G* denotes the Gibb's free energy of the state designated by subscripts of H (high-temperature state) and L (low-temperature state). Since the volume fractions of the γ and γ′ phases are assumed to be identical, the Gibb's free energy of the low-temperature state is expressed as,

$$G_{\mathrm{L}} = \frac{1}{2}(G^{\gamma} + G^{\gamma'}) \tag{2}$$

The enthalpy of the relevant phase, *E*, is calculate as the sum of bonding energies among the constituent atoms and is expressed as,

$$E = \sum_{x,y} P_{xy}\varepsilon_{xy} \tag{3}$$

where P_{xy} and ε_{xy} are the probability for the existence of the *x*–*y* bond and the bonding energy of the *x*–*y* bond, respectively. The values of P_{xy} are expressed with the mole fractions of the relevant constituent elements and are calculated as,

$$P_{xx}^{\gamma} = C_x^2 \tag{4}$$

and

$$P_{xy}^{\gamma} = 2C_xC_y \tag{5}$$

for the γ (fcc disordered) phase, and are calculated as,

$$P_{xx}^{\gamma'} = \frac{1}{2}C_x^{A2} + \frac{1}{2}C_x^AC_x^B \tag{6}$$

and

$$P_{xy}^{\gamma'} = C_x^AC_y^A + \frac{1}{2}C_x^AC_y^B + \frac{1}{2}C_y^AC_x^B \tag{7}$$

for the γ′ ($L1_2$ ordered) phase, respectively. C_x, C_x^A and C_x^B denote the mole fractions of the element X in the disordered phase, in A-sites and in B-sites of the A_3B ordered phase, respectively. The configuration entropy of the relevant phase, *S*, is also expressed with the mole fractions of the constituent elements as,

$$S^{\gamma} = -R\sum_x C_x \ln C_x \tag{8}$$

and

$$S^{\gamma'} = -R\left(\frac{3}{4}\sum_x C_x^A \ln C_x^A + \frac{1}{4}\sum_x C_x^B \ln C_x^B\right) \tag{9}$$

for the γ (fcc disordered) and γ′ ($L1_2$ ordered) phases, respectively. The value of ΔG in (1) is expressed with the use of the ordering energy, $\tilde{\varepsilon}_{xy}$, and the entropy, *S*, in (4)–(9). The ordering energy is expressed as,

$$\tilde{\varepsilon}_{xy} = \varepsilon_{xy} - \frac{\varepsilon_{xx} + \varepsilon_{yy}}{2} \tag{10}$$

and typical values are compiled in the literature [10]. The values adopted in the present calculation are tabulated in Table 1.

Table 1
Ordering energy, $\tilde{\varepsilon}_{xy}$, taken from the literature [10]. The unit is kJ mol^{-1}.

y	x		
	Co	Al	W
Co	0	−43	−2
Sc	−44	−68	14
Ti	−42	−61	−9
V	−21	−40	−1
Cr	−7	−30	1
Mn	−8	−43	9
Fe	−1	−32	0
Ni	0	−48	−5
Y	−31	−69	35
Zr	−60	−83	−14
Nb	−37	−44	−13
Mo	−7	−24	0
Tc	0	−46	−10
Ru	−1	−48	−15
Rh	−3	−64	−14
Pd	−2	−84	−10
La	−24	−68	46
Hf	−51	−75	−10
Ta	−36	−46	−11
Re	3	−30	−6
Os	0	−43	−15
Ir	−5	−60	−23
Pt	−11	−82	−30

3.2. Results of calculations

γ′ solvus temperatures calculated for the ternary alloy (Co–9 at.%Al–7 at.%W) and quaternary alloys with three different cases in terms of the partitioning and site occupancy behavior are tabulated in Table 2. Calculated γ′ solvus temperatures for quaternary alloys are reduced in most cases when compared with that of the ternary alloy. One of the reasons for this is that the volume fractions of the γ and γ′ phases are assumed to be unchanged upon quaternary alloying and to be identical with each other, which is different from what is observed in experiments, as described later in Section 4. In fact, the γ′ solvus temperature of the Co–9 at.%Al–9 at.%W alloy thus calculated assuming the identical volume fractions for the γ and γ′ phases is 320 K, which is lower than that (380 K) calculated for the Co–9 at.%Al–7 at.%W alloy.

Table 2
γ′ solvus temperatures calculated for the ternary alloy (Co–9 at.%Al–7 at.%W) and quaternary alloys with three different partitioning and site occupancy behaviors. The temperature in bold style indicates the highest one. The unit is K.

X	γ phase	A-site of γ′ phase	B-site of γ′ phase
–	380		
Sc	384	223	**390**
Ti	364	261	**366**
V	**363**	290	343
Cr	**360**	317	316
Mn	**367**	310	308
Fe	**357**	336	292
Ni	353	**358**	257
Y	**397**	224	373
Zr	366	236	**383**
Nb	359	269	**373**
Mo	**359**	315	325
Tc	348	**365**	254
Ru	344	**372**	248
Rh	346	**376**	230
Pd	349	**386**	199
La	**403**	225	366
Hf	366	248	**372**
Ta	360	270	**369**
Re	350	**355**	275
Os	344	**371**	253
Ir	339	**382**	231
Pt	336	**393**	207

However, once the realistic volume fractions for the two phases (20%:80% for γ:γ′) are taken into account, the γ′ solvus temperature of the former alloy is calculated to increase to 394 K. In addition, all γ′ solvus temperatures tabulated in Table 2 are considerably lower than that (1273 K) experimentally observed for Co–Al–W ternary alloys [1]. A part of this discrepancy comes from the small ordering energy between Co and W, $\tilde{\varepsilon}_{Co,W}$ (see Table 1), though there are intermetallic compounds with considerably high decomposition temperatures in Co rich side. It is expected that the solvus temperature is calculated more closed to the actual temperature, if suitable ordering energy is applied. These indicate that the variation of the γ′ solvus temperature upon quaternary alloying cannot be described quantitatively with the present calculation and will be discussed only qualitatively, paying attention to the relative change in the γ′ solvus temperature with respect to that for the Co–9 at.%Al–7 at.%W ternary alloy.

For each of quaternary alloying elements, the γ′ solvus temperature varies with the partitioning and site occupancy behavior (i.e., depending on whether the quaternary element is in the disordered phase, in A-sites and or in B-sites of the A_3B ordered phase). Of the three different γ′ solvus temperatures calculated for three different cases of the partitioning and site occupancy behavior of a particular quaternary alloying element, one exhibiting the highest temperature (indicated with bold letters in Table 2) is taken to be the γ′ solvus temperature of the relevant quaternary element. This is due to the fact that, of the three different low-temperature states corresponding to the three different cases of the partitioning and site occupancy behavior, the low-temperature state that exhibits the lowest Gibb's free energy is expected to give rise to the highest γ′ solvus temperature, which corresponds to the intersection of the Gibb's free energy curves of the high- and low-temperature states, as schematically shown in Fig. 1. Thus, the most stable partitioning and site occupancy behavior for quaternary alloying elements corresponds to that indicated with bold letters in Table 2 (i.e., with the highest calculated γ′ solvus temperature). The calculated partitioning and site occupancy behaviors for quaternary alloying elements are classified roughly into four cases, depending on the ordering tendency of the relevant quaternary element with Co and W. If the ordering tendency of the relevant quaternary element with Co is high (a large negative value for the ordering energy), the relevant quaternary element tends to be partitioned more in the disordered

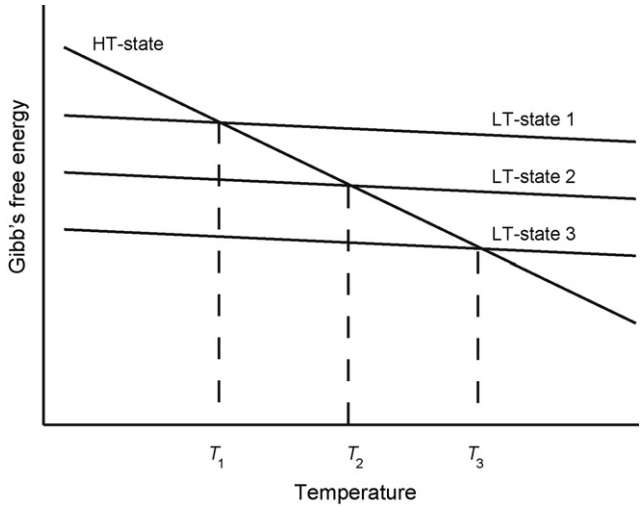

Fig. 1. Schematic illustration of Gibb's free energy-temperature curves for the high-temperature (fcc disordered) state and three different low-temperature states. The intersections of the Gibb's free energy curves of the high- and low-temperature states correspond to the expected γ′ solvus temperatures for three different cases of the low-temperature state.

phase when the phase-separation tendency of the relevant quaternary element with W is high (a large positive value for the ordering energy) (La and Y) while when the phase-separation tendency of the relevant quaternary element with W is not so high, it tends to occupy B-sites of the A_3B ordered phase (Sc, Zr, Nb, Ta, Ti and so on). If the ordering tendency of the relevant quaternary element with Co is not high (with a value for the ordering energy close to zero), on the other hand, the relevant quaternary element tends to occupy A-sites of the A_3B ordered phase when the ordering tendency of the relevant quaternary element with W is high (a large negative value for the ordering energy) (Pt, Pd, Ni, Re and so on) while it tends to be partitioned more in the disordered phase when the ordering tendency of the relevant quaternary element with W is not so high (Mn, V, Cr, Fe and so on).

The γ′ solvus temperature is calculated to vary with the partitioning and site occupancy behavior of quaternary elements and the general tendency calculated is summarized below. When the quaternary element is partitioned more in the disordered phase, the γ′ solvus temperature tends to increase as the phase-separation tendency of the quaternary element with W increases (i.e., as the ordering energy of the relevant quaternary element with W increases in positive values). When the quaternary element occupies A-sites of the A_3B ordered phase, the γ′ solvus temperature tends to increase as the ordering tendency of the quaternary element with W and Al increases (i.e., as the ordering energies of the relevant quaternary element with W and Al increase in negative values). On the other hand, when the quaternary element occupies B-sites of the A_3B ordered phase, the γ′ solvus temperature tends to increase as the ordering tendency of the relevant quaternary element with W and Al increases given the high ordering tendency with Co.

4. Microstructures and thermo-mechanical analysis

4.1. Ternary alloys

Fig. 2(a)–(c) shows SEM back-scattered electron (BSE) images of Co–9 at.%Al–*x* at.%W ternary alloys with *x* = 6, 7 and 8, respectively. Bright areas correspond to the γ′ phase forming cuboidal precipitates aligned along ⟨1 0 0⟩, as previously reported [1]. The volume fraction of the γ′ phase linearly increases with the increase in the W content, as tabulated in Table 3. From the variation of the volume fraction of the γ′ phase with the W content and EDS analysis, the W content in the γ and γ′ phases coexisting with each other are estimated as 3.5 and 10.5 at.%, respectively. This agrees well with the previously reported phase diagram [1]. Since the volume fraction of the γ′ phase in the Co–9 at.%Al–7 at.%W alloy is closed to 50%, we have selected the alloy as the base alloy for investigating the influence of quaternary elements on the γ′ solvus temperature.

Table 3
Volume fraction of the γ′ phase and γ′ solvus temperature of Co–9 at.%Al–*x* at.%W ternary alloys.

Composition, *x*	6	7	8
Volume fraction of the γ′ phase, $V_{f\gamma'}$ (%)	36	49	64
γ′ solvus temperature, T_s (K)	1221	1238	1258

Values of relative elongation with respect to the original specimen length at room temperature are plotted in Fig. 3(a) for Co–9 at.%Al–*x* at.%W ternary alloys with *x* = 6, 7 and 8. Values of coefficient for thermal expansion (CTE) are derived in Fig. 3(b) as the first derivatives of the curves in Fig. 3(a). The values of CTE for these three alloys are about 1.35×10^{-5}/K at low temperatures. For all three alloys, the value of CTE gradually increases with increasing temperature below 800 K. This is due to the fact that the volume fraction of the γ′ phase decreases with increasing temperature. Once the γ′ phase dissolved in the γ phase at high temperatures, the value of CTE suddenly decreases to the value of about 1.70×10^{-5}/K. The γ′ solvus temperature is determined as the temperature at which the value of CTE discontinuously changes as indicated by arrows in Fig. 3. The γ′ solvus temperature thus determined tends to increase as the W content increases (i.e., the volume fraction of the γ′ phase increases), as tabulated in Table 3.

4.2. Quaternary alloys

Values of relative elongation with respect to the original specimen length at room temperature and values of CTE are plotted in Fig. 4(a) and (b) as a function of temperature for some selected quaternary Co–9 at.%Al–7 at.%W–2 at.%X alloys. The γ′ solvus temperature is determined as the temperature at which the value of CTE discontinuously changes, as in the case of ternary alloys. For the Sc-containing alloy, the γ′ solvus temperature is observed to increase to 1257 K. The discontinuity observed at about 1427 K in the CTE-temperature curves for the Sc-containing alloy indicated by a double arrow in Fig. 4 is attributed to the dissolution of precipitates of the third phase in the γ phase from microstructure observations, as described later. The dissolution of precipitates of the third phase in the γ phase at high temperatures is similarly observed for Zr- and Hf-containing alloys. The γ′ solvus temperatures are determined to increase to 1258 and 1343 K for V- and Ta-containing alloys, respectively. The γ′ solvus temperatures thus determined by thermo-mechanical analysis for Co–9 at.%Al–7 at.%W–2 at.%X quaternary alloys are summarized in Table 4. The γ′ solvus tem-

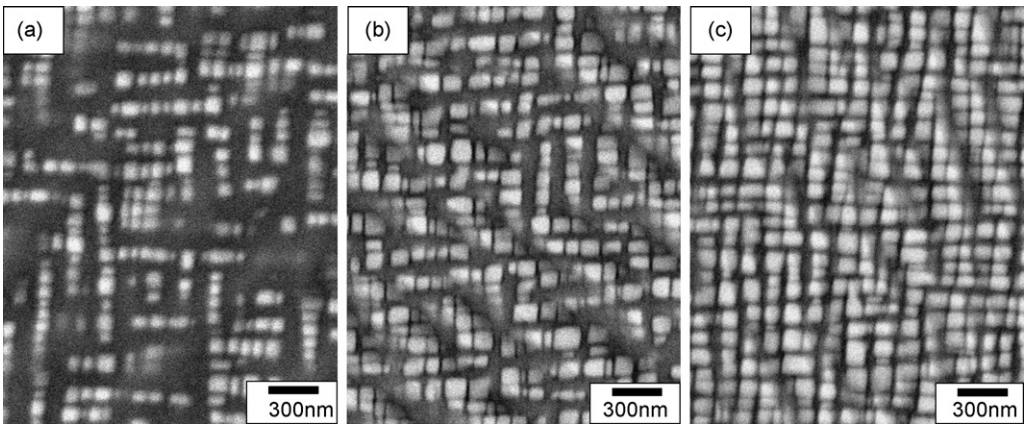

Fig. 2. SEM back-scattered electron images of Co–9 at.%Al–*x* at.%W ternary alloys with *x* = (a) 6, (b) 7 and (c) 8.

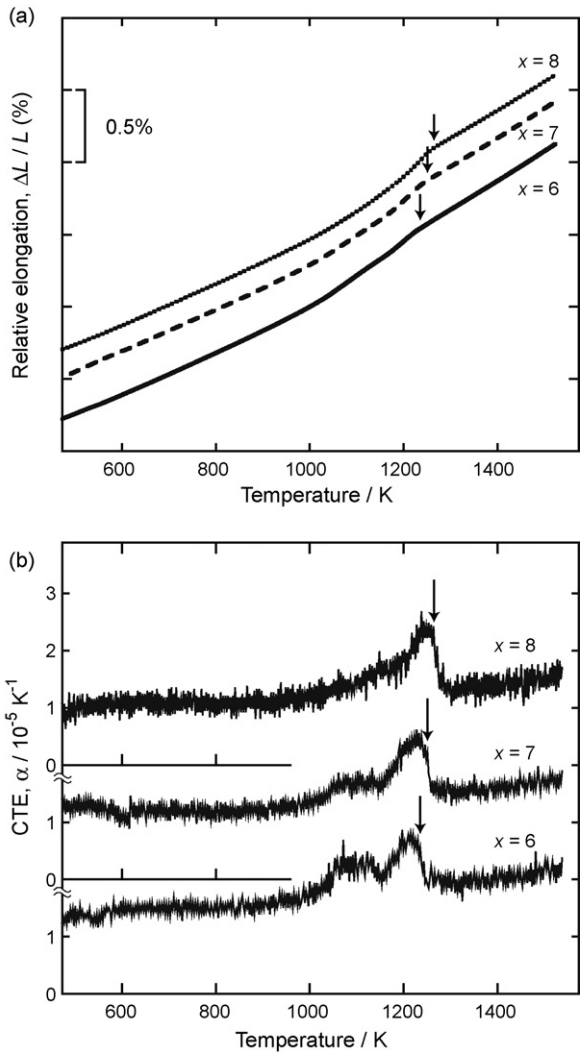

Fig. 3. (a) Values of relative elongation with respect to the original specimen length at room temperature plotted as a function of temperature for Co–9 at.%Al–*x* at.%W ternary alloys with *x* = 6, 7 and 8. (b) Coefficient for thermal expansion derived as the first derivatives of the curves in (a).

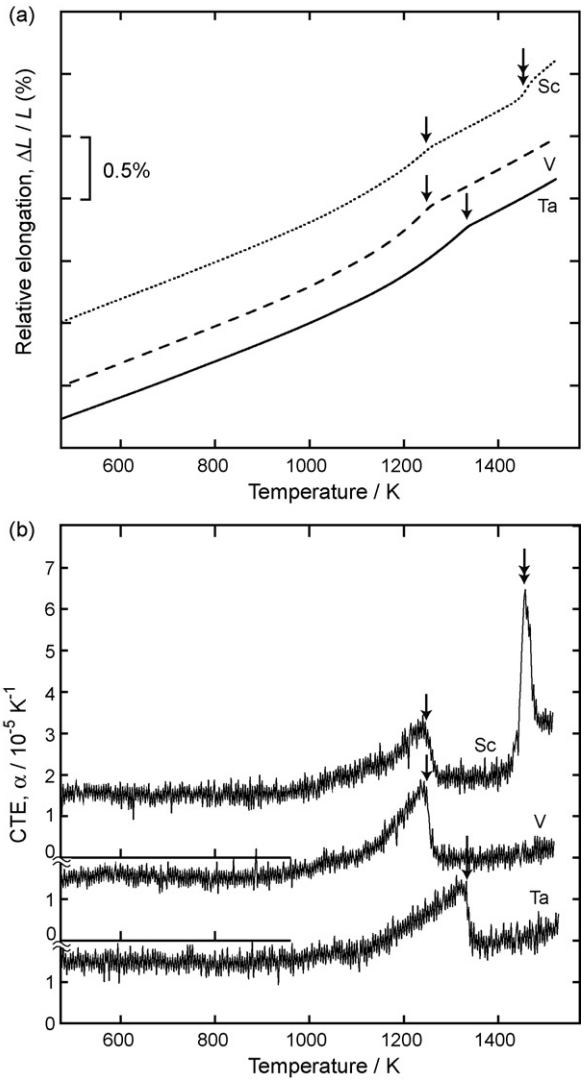

Fig. 4. (a) Values of relative elongation with respect to the original specimen length at room temperature plotted as a function of temperature for some selected Co–9 at.%Al–7 at.%W–2 at.%X quaternary alloys. Coefficient for thermal expansion derived as the first derivatives of the curves in (a).

peratures for most of these quaternary alloys are higher than that for the Co–9 at.%Al–7 at.%W ternary alloy, except for Re- and Fe-containing alloys.

SEM back-scattered electron images of Co–9 at.%Al–7 at.%W–2 at.%X quaternary alloys with X = Sc, Hf and Zr are illustrated in Fig. 5(a)–(c), respectively. These quaternary elements are calculated to occupy B-sites of the A_3B ordered phase increasing the γ′ solvus temperatures, since their ordering tendency with Co is high and their phase-separation tendency with W is not so high. However, their strong ordering tendency with Co has forced the corresponding quaternary alloys to form a significant volume fraction of the third phase consisting mainly of Co and the relevant quaternary element and the solid-solubility of the quaternary elements in the γ and γ′ phases are both negligibly small. This is the reason why the increase in the γ′ solvus temperature upon alloying these elements is not so high, in contrast to the expectation from thermodynamic calculation.

However, if the ordering tendency with Co is a little reduced, the formation of precipitates of the third phase is largely avoided and two-phase microstructures consisting of the γ and γ′ phases are formed upon alloying with quaternary elements such as Nb, Ta and Ti, as shown in Fig. 6(a)–(c). Upon alloying with these quaternary elements, the volume fraction of the γ′ phase increases (see Table 4), indicating that these elements are partitioned more in the γ′ phase. This is consistent with the results of calculation that these elements occupy B-sites of the A_3B ordered phase.

SEM back-scattered electron images of Co–9 at.%Al–7 at.%W–2 at.%X quaternary alloys with X = Ni and Re are illustrated in Fig. 7(a) and (b), respectively. Two-phase microstructures consisting of the γ and γ′ phases are formed upon alloying with these quaternary elements without any significant amount of the third phase. These quaternary elements are calculated to occupy A-sites

Table 4
Volume fraction of the γ′ phase and γ′ solvus temperatures determined by thermo-mechanical analysis for Co–9 at.%Al–7 at.%W–2 at.%X quaternary alloys.

Quaternary element, X	Ta	Mo	Nb	V	Re	Ti	Cr	Fe	Ni
Volume fraction of the γ′ phase, $V_{f\gamma'}$ (%)	65	44	54	56	41	61	39	35	45
γ′ solvus temperature, T_s (K)	1343	1250	1303	1258	1226	1293	1244	1231	1239

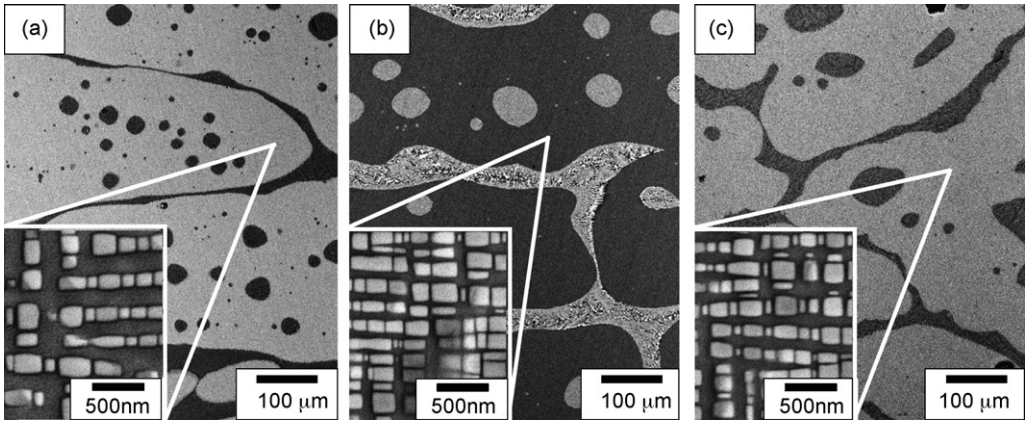

Fig. 5. SEM back-scattered electron images of Co–9 at.%Al–7 at.%W–2 at.%X quaternary alloys with X = (a) Sc, (b) Hf and (c) Zr.

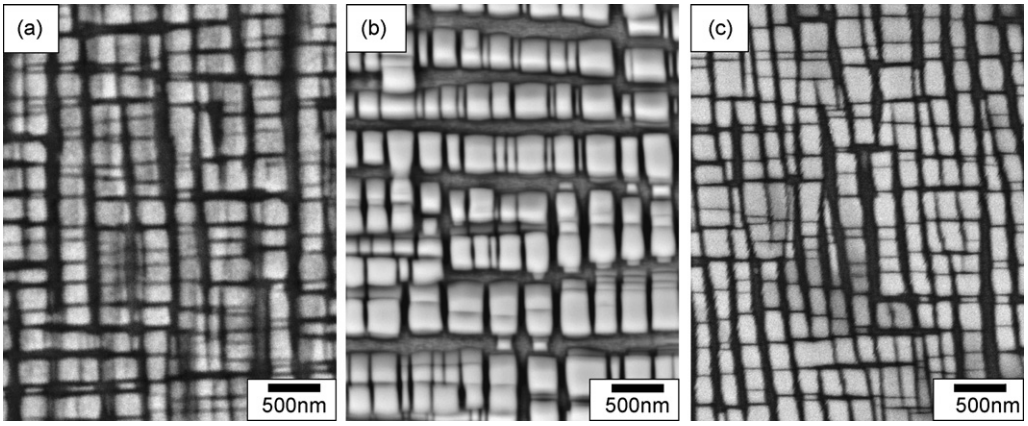

Fig. 6. SEM back-scattered electron images of Co–9 at.%Al–7 at.%W–2 at.%X quaternary alloys with X = (a) Nb, (b) Ta and (c) Ti.

of the A_3B ordered phase, since their ordering tendency with Co is not so high but that with W is high. In contrast to the expectation from thermodynamic calculation, these elements are found to be partitioned more in the γ phase when judged from the reduced volume fraction of the γ′ phase (Table 4). This is attributable to the fact that the difference between the γ′ solvus temperature when they are assumed to be in the γ phase and that when they are assumed to occupy A-sites in the γ′ phase is very small for these two elements (Table 2).

SEM back-scattered electron images of Co–9 at.%Al–7 at.%W–2 at.%X quaternary alloys with X = (a) Fe, (b) V, (c) Cr and (d) Mo are depicted in Fig. 8(a)–(d), respectively. Two-phase microstructures consisting of the γ and γ′ phases are formed upon alloying with these quaternary elements, except for Mo where a small volume fraction of Co_3W is observed as the third phase. The reason for this is not clear yet. These quaternary elements are calculated to be partitioned more in the γ phase, since their ordering tendencies with Co and W are not so high. These elements are indeed found to be partitioned more in the γ phase when judged from the reduced volume fraction of the γ′ phase (Table 4), except for V. V is found to be partitioned more in the γ′ phase, in contrast to the expectation from calculation. The reason for this has yet to be clarified.

Ti, V, Nb and Ta, which are well known as γ′ forming elements in nickel-based superalloys, act as γ′ forming elements also in Co-based alloys, increasing the γ′ solvus temperature effectively. On

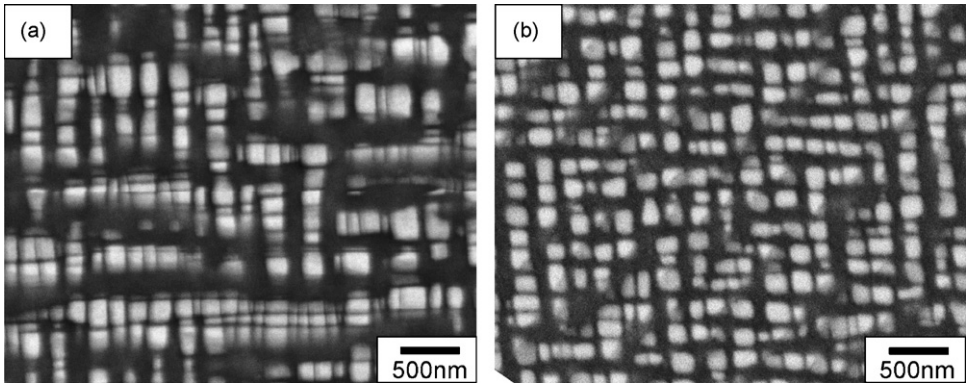

Fig. 7. SEM back-scattered electron images of Co–9 at.%Al–7 at.%W–2 at.%X quaternary alloys with X = (a) Ni and (b) Re.

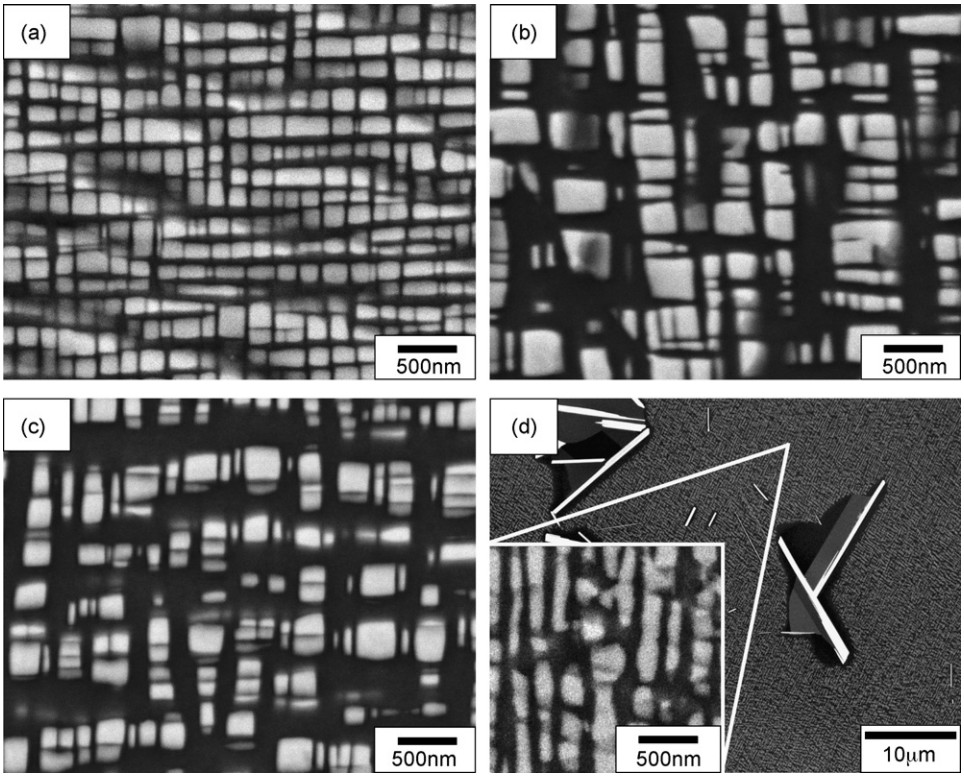

Fig. 8. SEM back-scattered electron images of Co–9 at.%Al–7 at.%W–2 at.%X quaternary alloys with X = (a) Fe, (b) V, (c) Cr and (d) Mo.

the other hand, other elements such as Cr, Fe, Ni, Mo and Re are partitioned more in the γ phase, reducing the volume fraction of the γ′ phase, and therefore, the increase in the γ′ solvus temperature is not significant.

5. Discussion

The comparison of the experimental results with those of theoretical thermodynamic calculation in terms of the partitioning and site occupancy behavior and the γ′ solvus temperature is summarized in Table 5. In Table 5, quaternary elements are arranged in the decreasing order of the γ′ solvus temperature deduced by thermodynamic calculation, except for Sc, Zr and Hf, for which a significant volume fraction of the third phase is formed. Except for these three elements, the order of the γ′ solvus temperature determined by experiment agree well with that deduced by thermodynamic calculation, as the order determined by experiment is indicated with the number in parentheses. The partitioning behavior predicted by thermodynamic calculation also agrees well with that determined by experiment, except for V, Ni and Re. As described previously, while the reason for this is not clear yet for V, the difference between the γ′ solvus temperature when Ni or Re are assumed to be in the γ phase and that when assumed to occupy A-sites in the γ′ phase is very small for these two elements (Table 2). The fair agreement between experiment and thermodynamic calculation summarized in Table 5 clearly indicates that basic thermodynamic calculation is useful to predict the variation of the γ′ solvus temperature of Co–Al–W based alloys with quaternary elements. As seen in Table 5, Nb, Ta and Ti are predicted to significantly increase the γ′ solvus temperature of Co–Al–W based alloys. This is also consistent with the experimental result by Omori et al. [9]. These elements have a common characteristic that they are γ′ forming elements (occupying B-sites of the A_3B ordered phase) that increase the volume fraction of the γ′ phase. This obviously stems from their thermodynamic characteristics that the ordering tendency with Co is high (but not significantly) and the phase-separation tendency with W is not so high. Although the γ′ solvus temperatures upon alloying with Sc, Zr and Hf are calculated to be high, this is not realized because of the formation of the third phase due to the too high ordering tendency with Co. Note that the partitioning of quaternary elements in a real system cannot be classified to the simple three cases applied to the present calculation (assumption iv); the values of partitioning coefficient for the sites may have a

Table 5
Comparison of the experimental results with the results of thermodynamic calculation. Quaternary elements are arranged in the decreasing order of the γ′ solvus temperature deduced by thermodynamic calculation, except for Sc, Zr and Hf, for which a significant volume fraction of the third phase is formed. The numbers in parentheses indicate the order of the γ′ solvus temperature determined by experiment.

Quaternary element	Site occupation from theoretical calculation	Experimental results	γ′ solvus temperature/K	
			Theoretical calculation	Experimental results
Sc	B-site of γ′ phase	Precipitate other compounds	390	1257
Zr			383	1254
Hf			372	1275
Nb	B-site of γ′ phase	γ′ former	373	1303 (2)
Ta			369	1343 (1)
Ti			366	1293 (3)
V	γ phase	γ′ former	363	1258 (4)
Cr	γ phase	γ former	360	1244 (6)
Mo			359	1250 (5)
Fe			357	1231 (8)
Ni	A-site of γ′ phase	γ former	358	1239 (7)
Re			355	1226 (9)

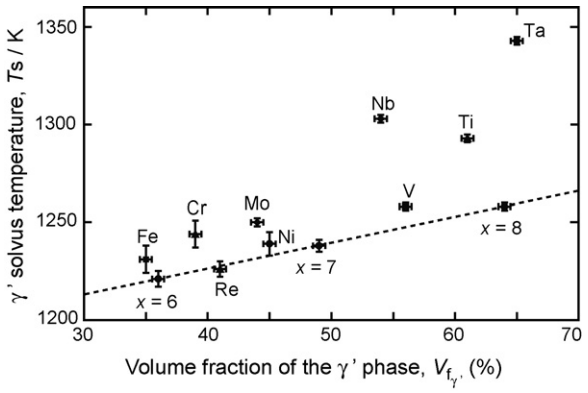

Fig. 9. Experimentally determined γ′ solvus temperature plotted as a function of the volume fraction of the γ′ phase.

fractional value. Since the magnitude of the increase or decrease the solvus temperature calculated varies with the partitioning behavior, detailed discussion in the magnitude of the change is difficult. Though the difficulty also comes from the uncertainty of the ordering energy, the trend of the change in the solvus temperature is well represented by the generalized ordering energies.

As is generally believed, the γ′ solvus temperatures of Co–Al–W based alloys vary with the volume fraction of the γ′ phase in the γ/γ′ two-phase field. For example, the γ′ solvus temperatures of Co–9 at.%Al–*x* at.%W ternary alloys vary from 1221 to 1258 K when the value of *x* changes from 6 to 8. The γ′ solvus temperatures determined for ternary and quaternary alloys are thus plotted in Fig. 9 as a function of the volume fraction of the γ′ phase. The dotted line in Fig. 9 indicates the variation of the γ′ solvus temperature with the volume fraction of the γ′ phase for the Co–9 at.%Al–*x* at.%W base ternary alloys. The efficiency of each of quaternary elements to increase the γ′ solvus temperature is then evaluated as the magnitude of the deviation from the dotted line at the corresponding volume fraction of the γ′ phase. This indicates that except for Re, all quaternary elements increase the γ′ solvus temperatures of Co–Al–W based alloys, with varying efficiencies depending on them. Of the quaternary elements investigated, Ta is observed to be the most effective element in increasing the γ′ solvus temperature. Nb and Ti are also observed to be very effective.

The γ′ solvus temperature of Co–Al–W based alloys is expected to increase as the amount of these elements in the γ/γ′ two-phase field increases. However, this is, off course, limited by the solid-solubility of these elements. In order to increase their solid-solubility in the γ/γ′ two-phase field, two different approaches are considered. One is to change the composition of the Co–Al–W base alloy so as to make the volume fraction of the γ′ phase in the ternary state small. This is achieved by reducing the W content, as seen in Fig. 9. Since these effective elements are γ′ formers that increase the volume fraction of the γ′ phase, there is a possibility to enlarge their solid-solubility by this approach. Another is to alloy with these effective elements together with a particular element that enlarges the solubility of these effective elements. Ni is indeed reported to enlarge the solubility of some transition metals [8]. These approaches to increase the γ′ solvus temperatures of Co–Al–W based alloys are currently under survey in our group.

6. Conclusions

(1) Basic thermodynamic calculation is proved to be useful in predicting the variation of the γ′ solvus temperature of Co–Al–W based alloys with quaternary elements when judged from the fact that the γ′ solvus temperature and partitioning behavior predicted by thermodynamic calculation agree well with those experimentally determined.
(2) All investigated quaternary elements, except for Re, increase the γ′ solvus temperatures of Co–Al–W based alloys with varying efficiencies depending on them. Nb, Ta and Ti are predicted to significantly increase the γ′ solvus temperature of Co–Al–W based alloys and this is indeed experimentally verified.
(3) These elements (Nb, Ta and Ti) effective in increasing the γ′ solvus temperature of Co–Al–W based alloys have a common characteristic that they are γ′ forming elements (occupying B-sites of the A_3B ordered phase) that increase the volume fraction of the γ′ phase. This obviously stems from their thermodynamic characteristics that the ordering tendency with Co is high (but not significantly) and the phase-separation tendency with W is not so high.

Acknowledgments

This work was supported by Grant-in-Aid for Scientific Research (A) from the Ministry of Education, Culture, Sports, Science and Technology (MEXT), Japan, and in part by the Global COE (Center of Excellence) Program of International Center for Integrated Research and Advanced Education in Materials Science from the MEXT, Japan.

References

[1] J. Sato, T. Omori, K. Oikawa, I. Ohnuma, R. Kainuma, K. Ishida, Science 312 (2006) 90–92.
[2] M. Osaki, S. Ueta, T. Shimizu, T. Omori, K. Ishida, Electr. Furnace Steel 79 (2008) 197–205.
[3] A. Suzuki, G.C. DeNolf, T.M. Pollock, Scr. Mater. 56 (2007) 385–388.
[4] A. Suzuki, T.M. Pollock, Acta Mater. 56 (2008) 1288–1297.
[5] S. Miura, K. Ohkubo, T. Mohri, Mater. Trans. 48 (2007) 2403–2408.
[6] K. Tanaka, T. Ohashi, K. Kishida, H. Inui, Appl. Phys. Lett. 91 (2007) 181907.
[7] B.C. Wilson, E.R. Cutler, G.E. Fuchs, Mater. Sci. Eng. A 479 (2008) 356–364.
[8] K. Shinagawa, T. Omori, J. Sato, K. Oikawa, I. Onuma, R. Kainuma, K. Ishida, Mater. Trans. 49 (2008) 1474–1479.
[9] T. Omori, J. Sato, K. Oikawa, I. Onuma, R. Kainuma, K. Ishida, Collected Abstract of the 2009 Spring Meeting of The Japan Institute of Metals, JIM, Sendai, 2009, p. 206.
[10] F.R. de Boer, R. Boom, W.C.M. Mattens, A.R. Miedema, A.K. Niessen, Cohesion in Metals, North-Holland, 1980.